Prediction of stress field in Japan using GPS network data

Muneo Hori[1], Toshio Kameda[2], and Teruyuki Kato[1]

[1]*Earthquake Research Institute, University of Tokyo, Bunkyo, Tokyo 113-0032, Japan*
[2]*Department of Structural Engineering, Tsukuba University, Tennodai, Tsukuba 305-8577, Japan*

(Received January 11, 2000; Revised September 18, 2000; Accepted September 21, 2000)

The applicability of a new inversion method to the Japanese Islands is examined. This method can compute a self-equilibrating stress increment from a strain increment, and the validity of the method is verified for metal-like-materials. Some modifications will be needed in applying the new inversion method to the Japanese Islands when a strain increment measured by the GPS array is used as input data. In this paper, we try to compute the stress increment associated with a measured displacement increment. It is shown that the inversion works and the stress increment is computed. The validity of the results, however, cannot be verified right now. Some information on regional constitutive relations is obtained from the measured strain increment and the predicted stress increment. We discuss the applicability of the inversion method, and clarify modifications that are needed for more reliable prediction.

1. Introduction

The Geographycal Survey Institute of Japan (GSI) has been operating a nationwide Global Positioning System (GPS) array since 1994; see, for instance, Kato *et al.* (1998). While this array is aimed at monitoring crustal deformation, the data obtained can be used for the prediction of regional stress increments and constitutive relations by applying a suitable inversion method. As such a method, we adopt a new inversion method proposed by the authors (Hori and Kameda, 1998; Hori *et al.*, 1999). This method was originally developed to identify local stress and constitutive relations of a small sample of metal-like material, by measuring a distribution of strain on the sample surface.

While restricted to a two-dimensional plane state, a key feature of the new inversion method is that it can find three components of a stress increment using two equations of equilibrium and one condition determined by a measured displacement increment. A specific form of the constitutive relations needs not be assumed. This sounds strange since ordinary inversion methods estimate the parameters of assumed constitutive relations by minimizing the difference between measured data and computed displacement. However, the validity of the new inversion method is rigorously proved, and the practical usefulness is being checked by a numerical simulation and a model experiment; see Hori and Kameda (1998, 2000).

In this paper, we examine the applicability of the new inversion method to the Japanese Islands. Since the method is for elasto-plastic bodies, our present purpose is to examine whether the method can work to produce stress increments associated with measured displacement increments. The content of the paper is as follows: In Section 2, the basic formulation of the new inversion method is briefly presented, together with results of a numerical simulation. In Section 3, we apply the new inversion method to compute the stress increment implied by a strain increment measured by GPS during 1997 and 1998. We discuss the basic applicability of the new inversion method to the Japan Islands. Index notation is used in this paper and the summation convention is employed.

2. Formulation and Verification of Inversion Method

First, we clarify the problem setting. A thin body, V, consisting of an elasto-plastic material is considered. The following two assumptions are made: 1) the body is in a state of plane stress; and 2) displacement and traction, u_i and t_i, are measured on the surface S and the boundary ∂S, respectively; see Fig. 1. The elasto-plasticity means that the strain increment can be decomposed into elastic and plastic parts, i.e., $\dot{\epsilon}_{ij} = \dot{\epsilon}^{e}_{ij} + \dot{\epsilon}^{p}_{ij}$, where superscript e or p stands for the elastic or plastic part. The elastic strain increment is related to the stress increment through an elasticity tensor, c_{ijkl}, and the plastic strain rate is given as the gradient of a certain yield function. While the yield function is complicated, it is generally observed for metals that the plastic strain increment is incompressible. Hence, we make the third assumption of $\dot{\epsilon}^{p}_{11} + \dot{\epsilon}^{p}_{22} = 0$.

Now, we consider three in-plane stress components. The increments must satisfy the equilibrium,

$$\frac{\partial \dot{\sigma}_{11}}{\partial x_1} + \frac{\partial \dot{\sigma}_{12}}{\partial x_2} = 0, \quad \frac{\partial \dot{\sigma}_{12}}{\partial x_1} + \frac{\partial \dot{\sigma}_{22}}{\partial x_2} = 0. \tag{1}$$

It then follows from $\dot{\sigma}_{ij} = c_{ijkl}\dot{\epsilon}^{e}_{kl}$ that Eq. (1) and the assumption of $\dot{\epsilon}^{p}_{11} + \dot{\epsilon}^{p}_{22} = 0$ yield three equations for $\dot{\epsilon}^{p}_{ij}$. To

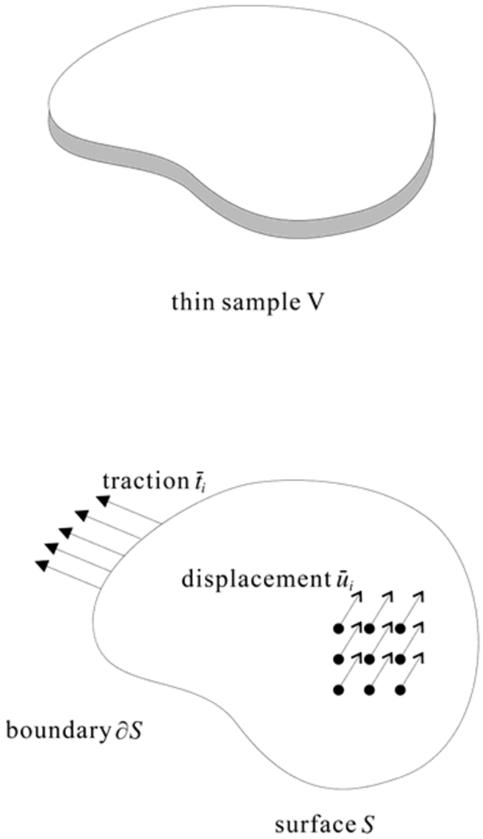

Fig. 1. Body in plane stress state.

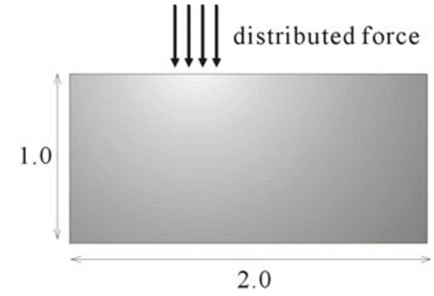

Fig. 2. Numerical simulation of material sample.

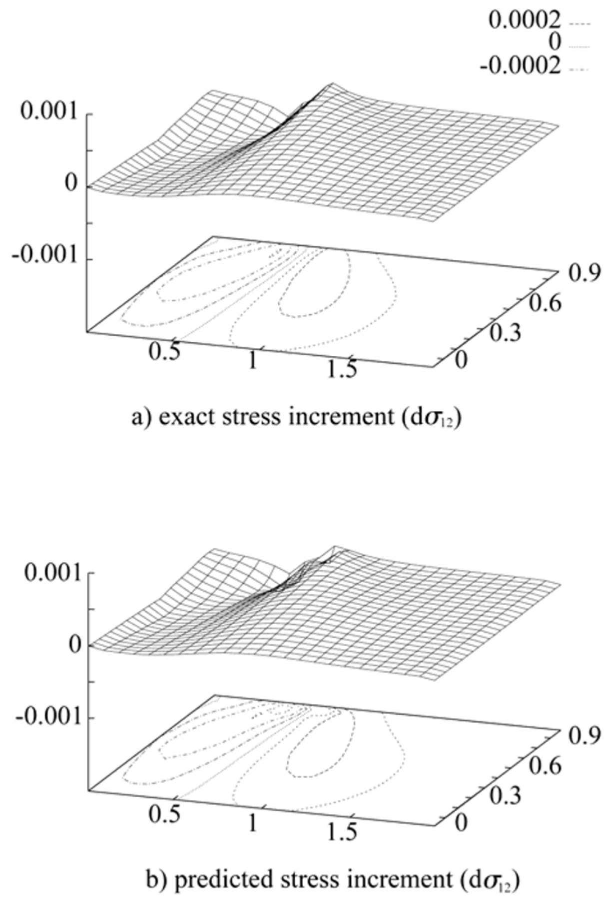

Fig. 3. Comparison of stress distribution.

simplify expression, we denote $\dot{\sigma}^*_{ij} = -\, c_{ijkl}\dot{\epsilon}^{\mathrm{p}}_{kl}$ and rewrite the three equations for $\dot{\epsilon}^{\mathrm{p}}_{ij}$ in terms of $\dot{\sigma}^*_{ij}$. When c_{ijkl} is isotropic,

$$\dot{\sigma}^*_{11} + \dot{\sigma}^*_{22} = 0 \tag{2}$$

is derived from $\dot{\epsilon}^{\mathrm{p}}_{11} + \dot{\epsilon}^{\mathrm{p}}_{22} = 0$, and Eq. (1) becomes differential equations for $\dot{\sigma}^*_{11} (= -\dot{\sigma}^*_{22})$ and $\dot{\sigma}^*_{12}$. Traction increment measured on the boundary prescribes boundary conditions. Thus, boundary value problems are posed for $\dot{\sigma}^*_{ij}$.

After some manipulation, the boundary value problem is decoupled, and two boundary value problems for $\dot{\sigma}^*_{11}$ and $\dot{\sigma}^*_{12}$ are derived. For instance, the problem for $\dot{\sigma}^*_{11}$ is

$$\begin{cases} \dfrac{\partial^2 \dot{\sigma}^*_{11}}{\partial x_1^2} + \dfrac{\partial^2 \dot{\sigma}^*_{11}}{\partial x_2^2} = -\dfrac{\partial^2 \dot{\sigma}^{\mathrm{a}}_{11}}{\partial x_1^2} + \dfrac{\partial^2 \dot{\sigma}^{\mathrm{a}}_{22}}{\partial x_2^2} \quad \text{on } S, \\[2ex] \dot{\sigma}^*_{11} = n_1\dot{t}_1 - n_2\dot{t}_2 - (n_1^2\dot{\sigma}^{\mathrm{a}}_{11} - n_2^2\dot{\sigma}^{\mathrm{a}}_{22}) \text{ along } \partial S, \end{cases} \tag{3}$$

where $\dot{\sigma}^{\mathrm{a}}_{ij}$ is the apparent stress increment that is computed by using strain increment as $\dot{\sigma}^{\mathrm{a}}_{ij} = c_{ijkl}\dot{\epsilon}_{kl}$. Equation (3) is linear and can be solved easily by numerical computation. Once $\dot{\sigma}^*_{ij}$'s are obtained, the stress increment is given as

$$\dot{\sigma}_{ij} = \dot{\sigma}^{\mathrm{a}}_{ij} + \dot{\sigma}^*_{ij}. \tag{4}$$

As an illustrative example, we present results of the numerical simulation by Hori *et al.* (1999), who studied a rectangular material sample subjected to distributed forces; see Fig. 2. Field variables such as displacement and traction were first computed, and then the new inversion method was applied to predict the stress increment using the computed displacement and traction increments as input data. It should be emphasized that no information about plastic constitutive relations was given although the elastic properties were known a-priori. In Fig. 3, the comparison of the predicted stress increment with the exact one is presented; a) and b) are the exact and predicted $\dot{\sigma}_{12}$. The agreement is satisfactory as the maximum relative error in predicting $\dot{\sigma}_{12}$ is less 1%, and the stress concentration near the load is almost the same. It is also shown that unknown plastic constitutive relations are well predicted by using the inverted stress and the measured data; see Hori *et al.* (1999).

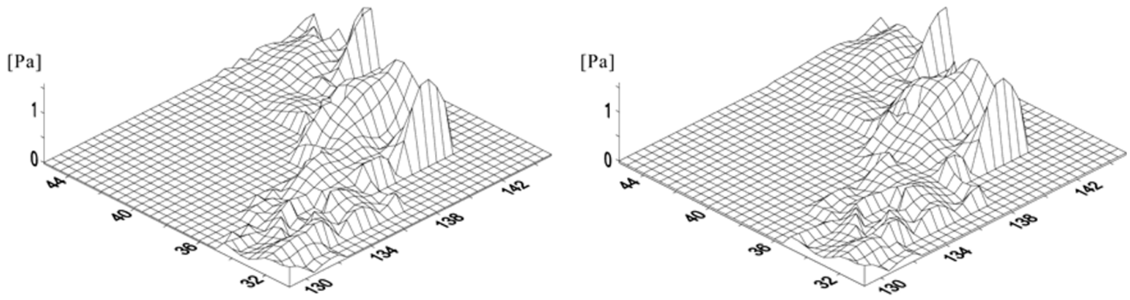

a) $\Delta=0.25$ b) $\Delta=0.125$

Fig. 4. Convergence of $\dot{\tau}$.

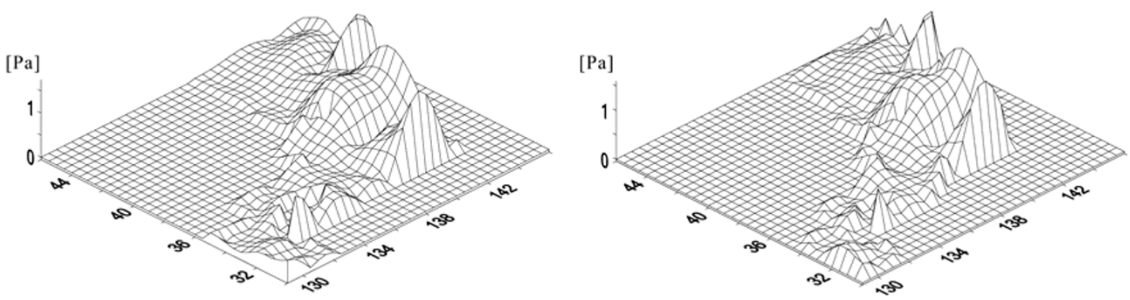

a) type 1 b) type 2

Fig. 5. Effects of boundary on $\dot{\tau}$.

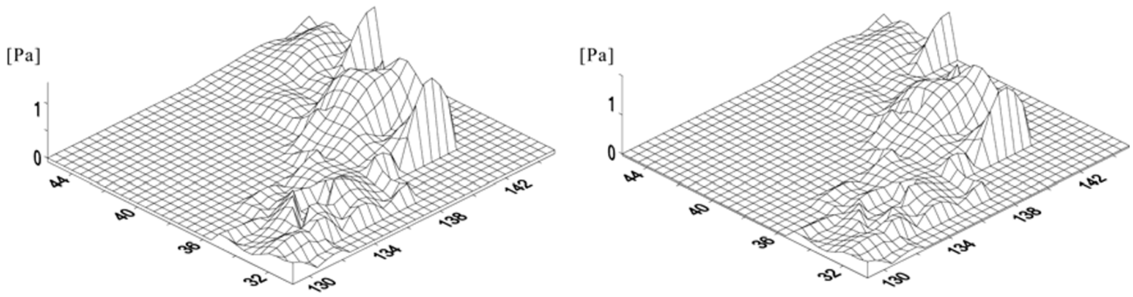

a) $\nu=0.2$ b) $\nu=0.3$

Fig. 6. Effects of reference elasticity on $\dot{\tau}$.

3. Application of Inversion Method to Japanse Islands

We examine the applicability of the new inversion method to the Japanese Islands, using a displacement increment measured by the nationwide GPS array. It should be emphasized that while the stress state of the Japanese Islands varies vertically, we may assume the plane stress state of the deformation during a period of the GPS measurement. This is because, in analyzing the deformation of the Japanese Islands during a short period, we can model the islands as a thin body which is subjected to the horizontal movement of the surrounding plates. Since the upper surface is traction free, the bottom surface is modeled as traction free as well. (The total stress, as a matter of course, is in equilibrium with the gravity force and hence vertical stress components cannot be neglected. For the stress increment, however, the vertical components are assumed to be much smaller than horizontal ones and hence are neglected.) We use the least squares prediction to get rid of measurement noises and to obtain a smooth distribution of the strain increment; see El-Fiky and Kato (1999a, b) for the least squares prediction. We use an isotropic reference elasticity of Young's modulus $E = 1$ [Pa] and Poisson's ratio $\nu = 0.25$.

In applying the new inversion method, we must pay some attention to the assumption of Eq. (2) and the boundary conditions. If inelastic deformation is due to the sliding of faults,

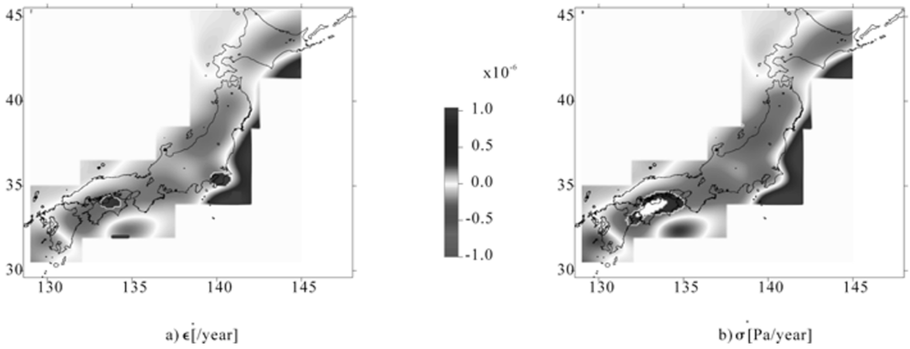

Fig. 7. Distribution of first invariant of strain and stress increment.

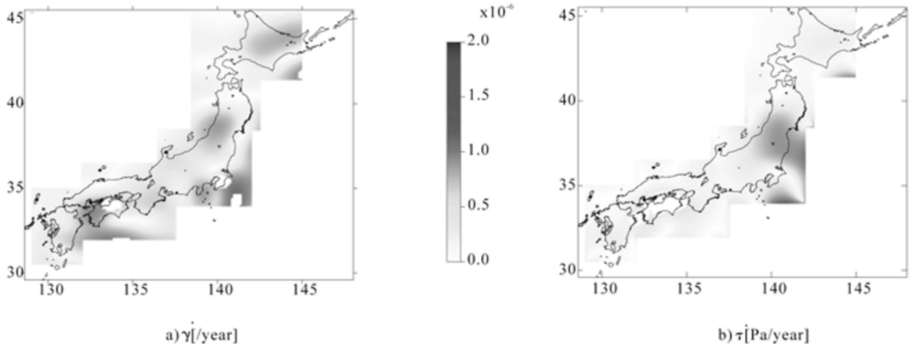

Fig. 8. Distribution of maximum shear and stress increment.

Eq. (2) holds since the sliding produces only shear deformation and the area change is zero; recall that Eq. (2) is derived from

$$\dot{\epsilon}^{\mathrm{p}}_{11} + \dot{\epsilon}^{\mathrm{p}}_{22} = 0.$$

It should be mentioned that the inversion method presented here can be applied if another condition beside Eq. (2) is assumed. For instance, the assumption of the local isotropy can be used as well, although the form of the boundary value problems is slightly modified; see Hori and Kameda (2000). The effects of unknown boundary traction can be treated separately in Eq. (3) due to the linearity of the boundary value problem, i.e., the solution is given by the sum of a stress increment satisfying the non-homogeneous equations and null boundary conditions and a stress increment satisfying homogeneous equations and the prescribed boundary conditions. The latter will produce a uniform stress increment if the boundary tractions are more or less uniform. In this analysis, therefore, we neglect the latter and compute only the former, i.e.,

$$\begin{cases} \dfrac{\partial^2 \dot{\sigma}^*_{11}}{\partial x_1^2} + \dfrac{\partial^2 \dot{\sigma}^*_{11}}{\partial x_2^2} = -\dfrac{\partial^2 \dot{\sigma}^{\mathrm{a}}_{11}}{\partial x_1^2} + \dfrac{\partial^2 \dot{\sigma}^{\mathrm{a}}_{22}}{\partial x_2^2} \text{ on } S, \\ \\ \dot{\sigma}^*_{11} = -(n_1^2 \dot{\sigma}^{\mathrm{a}}_{11} - n_2^2 \dot{\sigma}^{\mathrm{a}}_{22}) \qquad \text{along } \partial S. \end{cases}$$

First, we make three preliminary checks of the inversion method, solving the boundary value problems with a finite element method. The first check is the convergence of numerical solutions. In Fig. 4, we plot the maximum shear stress increment, $\dot{\tau}$, for different discretizations; a) and b) are for the element size of $\Delta = 0.25$ and 0.125 degree, respectively. The convergence is satisfactory as the relative difference between these two cases is around 1%. Second, we examine the effects of the boundary conditions. Two configurations of the domain are used, and zero tractions are prescribed on the boundary. The distribution of $\dot{\tau}$ is plotted in Fig. 5. It is seen that while there are some differences near the boundary, the distribution within the Japanese Islands is not much influenced by the boundary configurations. Finally, we compute the effects of the reference elasticity, c_{ijkl}, which computes apparent stress increment; unlike elasto-plastic metals, this elasticity cannot be determined for the Japanese Islands. Since isotropy is assumed, we change Poisson's ratio ν and plot the distribution of $\dot{\tau}$ in Fig. 6; a) and b) are for $\nu = 0.2$ and 0.3, respectively. Even though there are some differences

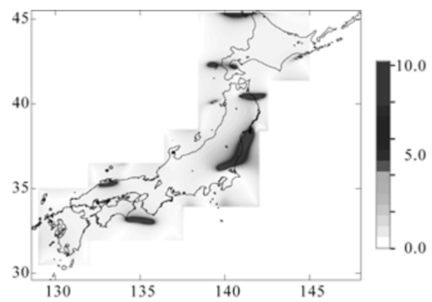

Fig. 9. Distribution of regional stiffness.

from place to place, the overall patterns are similar to each other. These preliminary checks support the applicability of the new inversion method to the Japanese Islands.

Now, we compute the stress increment fully, using the element size of $\Delta = 0.125$, the configuration of Type 1 shown in Fig. 5a) and Poisson's ratio of $\nu = 0.25$. In Figs. 7 and 8, we plot the distribution of the first invariant of strain and stress increment,

$$\dot{\epsilon} = \dot{\epsilon}_{11} + \dot{\epsilon}_{22}, \quad \dot{\sigma} = \dot{\sigma}_{11} + \dot{\sigma}_{22},$$

and the distribution of the maximum shear strain and stress increment,

$$\dot{\gamma} = \sqrt{(\dot{\epsilon}_{12})^2 + (\dot{\epsilon}_{11} - \dot{\epsilon}_{22})^2/4},$$
$$\dot{\tau} = \sqrt{(\dot{\sigma}_{12})^2 + (\dot{\sigma}_{11} - \dot{\sigma}_{22})^2/4},$$

respectively. The difference between the strain and stress increment distributions clearly show that, since the apparent stress increment does not satisfy equilibrium, non-zero $\dot{\sigma}^*_{ij}$ is generated and produces self-equilibrating stress increment. Since the strain and stress increments are obtained, we can consider regional constitutive relations. As an example, we plot the ratio of $\dot{\tau}$ to $\dot{\gamma}$, which is a measure of the regional shear stress, in Fig. 9. It is seen that there are regional heterogeneities.

Finally, we consider the applicability of the new inversion method to the Japanese Islands. In Figs. 7 and 9, high stress concentration near the boundary and some regions of quite large $\dot{\tau}/\dot{\gamma}$ are observed. These values are unrealistic, since this means that these regions have stiffness larger by an order of magnitude than nearby regions. They are probably due to the singularity of the solution of the differential equations at the corner and the failure of the assumption of Eq. (2). For unknown traction increment, some guess can be made by considering in-situ measurement of stress at several sites or by computing the stress increment that is associated with the overall crustal movement. The assumption of Eq. (2), however, should be replaced with a more general one. Also, we have to consider the least square prediction of displacement increment which may underestimate the regional particular deformation. In the present boundary value problem, however, higher order derivatives of displacement increment are computed and hence a smoother distribution is required. To resolve these two problems, Hori and Kameda (1999) are proposing several modification of the inversion method.

4. Concluding Remarks

The results of preliminary checks and trial computation support the basic applicability of the new inversion method to the Japanese Islands. While further investigation is definitely needed, it is seen that the new inversion method is potentially useful in predicting the stress increment. Drawbacks and limitations of the new inversion method are clarified, and rational modifications will be made for more reliable stress estimation. Once these drawbacks and limitations are resolved, the comparisons with known crust structures will be made to examine the validity of the new inversion method.

Acknowledgments. This research is supported partially by Grant-in-Aid for Scientific Research, the Ministry of Education, Science, Sports and Culture and partially by Japan Science and Technology Corporation.

References

El-Fiky, G. S. and T. Kato, Continuous distribution of the horizontal strain in the Tohoku district, Japan, deduced from least squares prediction, *J. of Geodyn.*, **27**, 213–236, 1999a.

El-Fiky, G. S. and T. Kato, Interplate coupling in the Tohoku district, Japan, deduced from geodetic data inversion, *J. Geophys. Res.*, **104**(B9), 20361–20377, 1999b.

Hori, M. and T. Kameda, Formulation of inverse problem of identifying material properties based on equivalent inclusion method, in *Proceeding of International Symposium on Inverse Problems*, edited by M. Tanaka and G. S. Dulikravich, pp. 225–234, Elsevier, New York, 1998.

Hori, M., T. Kameda, and N. Hosokawa, Formulation of identifying material property distribution based on equivalent inclusion method, *Structural Eng./Earthquake Eng.*, JSCE, **16**(1), 21–30, 1999.

Hori, M. and T. Kameda, Inversion of stress from strain without fully knowing constitutive relations, *J. Mech. Phys. Solids*, 2000 (in print).

Kato, T., G. S. El-Fiky, E. N. Oware, and S. Miyazaki, Crustal strains in the Japanese islands as deduced from dense GPS array, *Geophys. Res. Lett.*, **25**, 3445–3448, 1998.

M. Hori (e-mail: hori@eri.u-tokyo.ac.jp), T. Kameda, and T. Kato